Novel Power Smoothing Technique for a Hybrid AC-DC Microgrid Operating with Multiple Alternative Energy Sources

Pramod Bhat NEMPU[1], Jayalakshmi Narayana SABHAHIT[1], Dattatreya Narayan GAONKAR[2], Vidya Sudarshan RAO[3]
[1]*Department of Electrical and Electronics Engineering, Manipal Institute of Technology, Manipal Academy of Higher Education, Manipal, India - 576104*
[2]*Department of Electrical and Electronics Engineering, National Institute of Technology, Surathkal, Karnataka, India - 575025*
[3]*Department of Instrumentation and Control Engineering, Manipal Institute of Technology, Manipal Academy of Higher Education, Manipal, India – 576104*
jayalakshmi.ns@manipal.edu

***Abstract*—The power produced by renewable sources such as photovoltaic systems and wind energy conversion systems is highly intermittent due to continuously changing irradiance and wind velocity. When the distributed generation systems employing photovoltaic (PV) array and wind energy conversion system (WECS) operate in grid-tied mode, the power fluctuations affect the power quality of the grid. In a hybrid AC-DC microgrid (HMG), the dynamics of DC and AC subgrids influence each other. This paper proposes a supercapacitor based novel power smoothing methodology for the HMG with PV array, WECS, fuel cell (FC) and electrolyzer (EL) based hydrogen storage system considering the power fluctuations in both subgrids. The power smoothing technique on the DC subgrid aims to facilitate instantaneous power balance. The Kalman filter (KF) based velocity smoothing (KFV) approach is developed for the WECS. The KFV technique is compared with the power smoothing techniques presented in the literature. The KFV method is found to be effective in computing the smooth power reference for the supercapacitor system. By incorporating the proposed power smoothing technique in the HMG, the stress on the interlinking converter (ILC) and utility grid are minimized and the power quality is enhanced.**

***Index Terms*—Kalman filters, microgrids, power smoothing, renewable energy sources, supercapacitors.**

I. INTRODUCTION

The concept of microgrids employing non-conventional energy sources has drawn the attention of researchers recently. Sunlight and wind are freely available in nature and are harmless to the environment. The microgrid (MG) operates in grid-integrated mode and stand-alone mode. The HMG configuration is reliable compared to AC MGs and DC MGs. A HMG comprises both AC and DC subgrids [1, 2]. Power management within the subgrids, coordination among the subgrids and power quality issues are the challenges in a grid-tied HMG [3].

The permanent magnet synchronous generator (PMSG) based WECS is efficient due to the absence of gearbox [4]. An irradiance averaging technique for power smoothing of a PV system with BES is proposed in [5]. However, power smoothing is not clearly evaluated in the paper. The experimental investigation of the SC-based smoothing controller for the renewable energy-based DGs integrated with the low voltage grid is proposed in [6]. By monitoring the state of charge (SOC) of SC, appropriate smooth reference is provided for the SC system and the sliding mode controller is incorporated.

In [7], the power smoothing is investigated for a PV-BES hybrid system with different methods and SOC regulation is also accomplished. Various control approaches for power smoothing of WECS are reviewed in [8]. Energy storage based smoothing is expensive but efficient. A power smoothing controller for a WECS is developed with the combination of MPPT control and frequency deviation control loops. The gain of the supplementary control loop is adjusted for better smoothing performance [9]. This control scheme doesn't employ a storage system.

A novel power smoothing controller is proposed in [10] for a PV-WECS hybrid system using the battery. Efficient smoothing and SOC regulation of battery are achieved. An adaptive low pass filter (LPF) based power smoothing technique designed with a lithium-ion capacitor for PMSG based WECS in [11]. The comparative study of LPF and moving average methods using superconducting magnetic energy storage is presented in [12]. The LPF is proved to be effective. In [13], the authors proposed the power smoothing of WECS by wavelet transform. The authors inferred that wavelet transform based smoothing is efficient compared to the smoothing achieved with inertial filter.

The SC bank is incorporated for smoothing the output of the PV-WECS hybrid system. The fluctuating output of the PV array and WECS is processed by a rate limiter and then the average is computed to obtain smooth power reference in [14]. LPF is employed to achieve power smoothing in a PV system operating with the weak grid in [15]. The results presented show a reduction in total harmonic distortion (THD).

The analysis of WECS with SC during faults is described in [16]. During normal operation, the SC bank helps to mitigate the fluctuations in the power output of WECS. During the faults, SC absorbs power and helps to ride through the fault. The KF based weighted average approach is described in [17-18]. Various techniques for power

Digital Object Identifier 10.4316/AECE.2021.02011

smoothing of the PV system and WECS are reviewed in [19]. KF based weighted average approach is proved to be effective.

The research papers addressing power smoothing techniques in the literature have not considered the MGs with DC and AC subgrids. The effect of intermittent power generation from renewable sources on the operation of individual subgrids in HMG architecture is not addressed.

In this work, the PV system is the principal source in the DC subgrid and FC is the auxiliary source. The WECS is the only renewable source in the AC subgrid. Hence, the requirements for developing the power smoothing control schemes on two subgrids are different.

Therefore, this paper proposes the Kalman filter based control method for power smoothing of the WECS. For the DC subgrid, a simple power smoothing technique is developed so as to facilitate instantaneous power management by the SC as the FC and EL systems are controlled to achieve power balance. The research contributions of this article are as follows.

- KF based novel power smoothing technique is proposed for the WECS.
- The impact of intermittent power production from the PV system and WECS on individual subgrids in a HMG is analyzed and an appropriate power smoothing method is investigated to mitigate power fluctuations.

This paper is organized as follows. In section II, the configuration of the HMG is presented. In section III, different control schemes are described. The simulation results are analyzed in section IV. Conclusions are presented in section V.

II. CONFIGURATION OF HMG

The schematic illustration of the HMG is presented in Fig. 1. The main energy source on the DC subgrid is a PV array capable of producing 21 kW at standard conditions operating in MPPT mode. A 20 kW PMSG based WECS [14] is coupled to the AC bus, which is integrated with the utility grid. FC system of capacity 10 kW is chosen as the backup source in DC subgrid. EL system of rating 10 kW is used for energy storage. PV array is modelled based on the model described in [20]. Models of the FC stack and electrolyzer system are realized as described in [21-22]. The WECS consists of a rectifier and a boost converter. The output of the boost converter is inverted and delivered to the AC bus. AC bus is integrated with the grid through a 100 kVA transformer (415V/3.3kV). AC and DC subgrids are coupled by a bidirectional ILC and a filter [23]. The SC banks on both subgrids (SC1 and SC2) contain a series combination of 50 modules of rating 58 F and 16 V. The SC banks are controlled by bidirectional DC-DC converters.

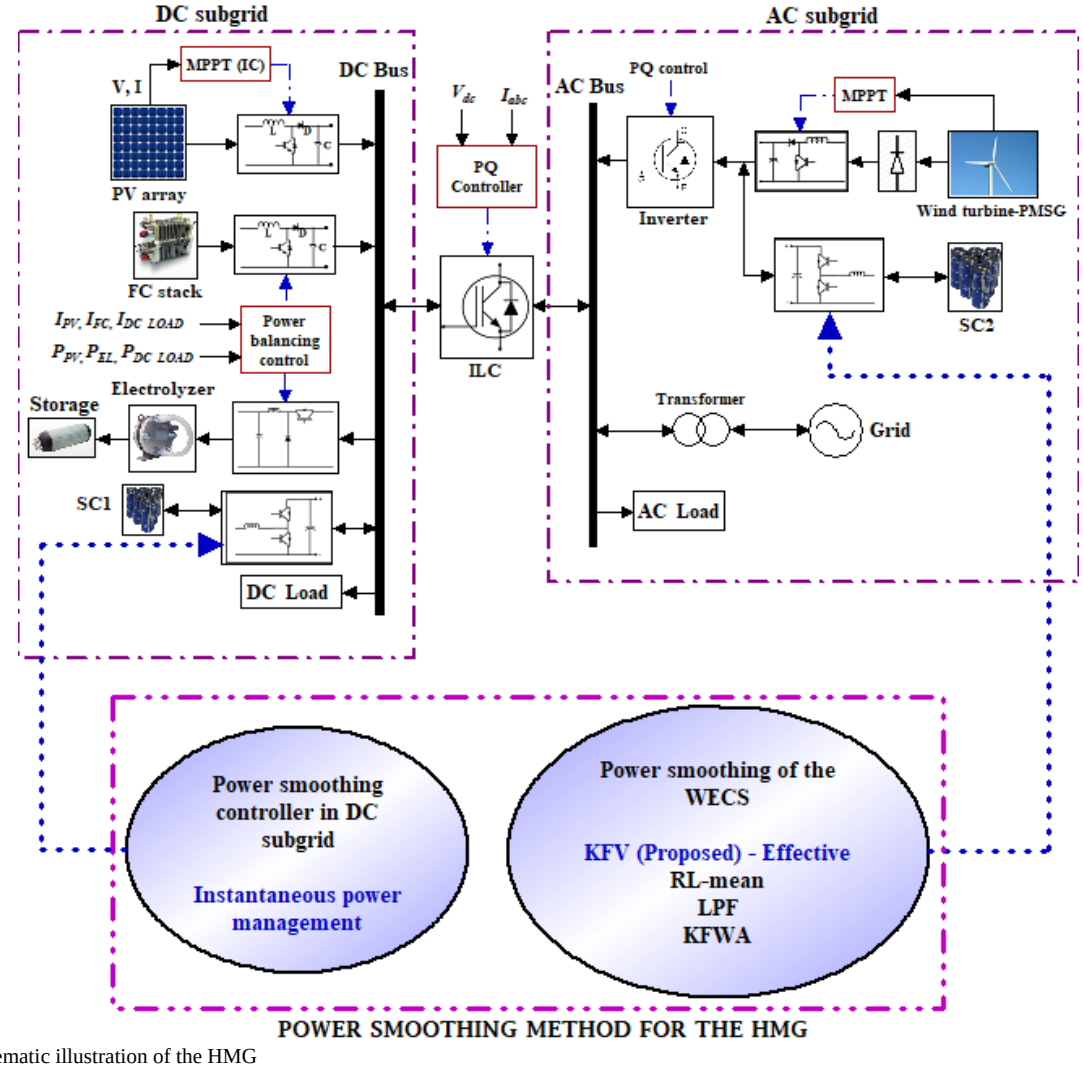

Figure 1. Schematic illustration of the HMG

III. Control Schemes

A. Control Schemes for the Power Balance of DC Subgrid

The control schemes of FC and EL systems realized for the power management in the DC bus are illustrated in Fig. 2. In the control strategy of the FC system, the difference between the DC load current ($I_{DC\ LOAD}$) and the current sensed at the output terminals of the PV system's converter (I_{PV}) is the reference signal. The current sensed from the output of the converter of the FC system (I_{FC}) is the feedback.

The difference between the power output of the PV array (P_{PV}) and DC load demand ($P_{DC\ LOAD}$) is the reference signal for the controller of the EL. The control strategies of both FC and EL systems employ the PI regulator. The FC system delivers power when the load demand on the DC bus goes beyond the output of the PV array. Surplus power generated is absorbed by the EL system (P_{EL}). Based on the current through the EL, hydrogen is produced, which is stored in a storage tank.

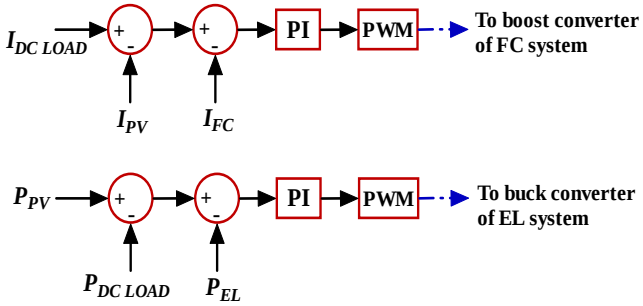

Figure 2. Control schemes of FC and EL systems

B. The Control Scheme of ILC

The DC subgrid is integrated with the AC subgrid through an ILC. The PQ control scheme [14] maintains the DC bus voltage (V_{dc}) at the desired value (800 V) and enables a proper exchange of power amongst the subgrids. The PQ controller of the ILC is shown in Fig. 3. The inverter of WECS is also regulated by a similar PQ control scheme.

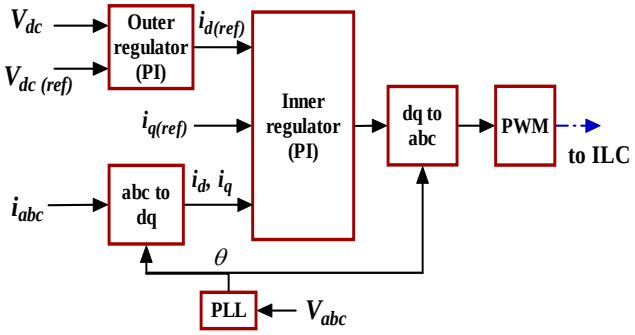

Figure 3. The PQ control scheme of ILC

The power in a three-phase network is given by equation (1):

$$P(t) = v_a i_a + v_b i_b + v_c i_c \tag{1}$$

Active and reactive power (P and Q) are computed based on d and q axis voltages v_d and v_q using the equations (2) and (3) respectively:

$$P = \frac{3}{2}\left(i_d v_d + i_q v_q\right) \tag{2}$$

$$Q = \frac{3}{2}\left(i_d v_q - i_q v_d\right) \tag{3}$$

When the reference frame and grid voltage are synchronized, P and Q can be expressed as per equations (4) and (5) respectively.

$$P = \frac{3}{2}(i_d v_d) \tag{4}$$

$$Q = \frac{3}{2}(i_q v_d) \tag{5}$$

where, i_d and i_q are the currents corresponding to the d and q axis. The outer loop of the control scheme maintains the DC bus voltage and the inner current control loop regulates i_d and i_q. The $i_{q\ (ref)}$ is made zero to ensure the operation at UPF. The phase-locked loop is used to measure the phase angle of grid voltage to synchronize ILC with the grid.

The voltage balance across the filter [24] is given by equation (6):

$$\begin{bmatrix} v_d^1 \\ v_q^1 \end{bmatrix} = R_f \begin{bmatrix} i_d \\ i_q \end{bmatrix} + L_f \frac{d}{dt}\begin{bmatrix} i_d \\ i_q \end{bmatrix} + L_f \begin{bmatrix} 0 & -\omega \\ \omega & 0 \end{bmatrix}\begin{bmatrix} i_d \\ i_q \end{bmatrix} + \begin{bmatrix} v_d \\ v_q \end{bmatrix} \tag{6}$$

where, L_f and R_f represent the total inductance and resistance of filter, respectively and ω is the angular frequency.

C. Power Smoothing in the DC Subgrid

The power smoothing controller on the DC subgrid is designed to provide or absorb power during sudden power variations in the DC bus. This control technique is depicted in Fig. 4. By incorporating the smoothing controller on the DC bus, power stress on the ILC can be minimized. When the power balance is disturbed by fluctuating load or generation, the controller decides the power to be absorbed or supplied by the SC1. A selection switch is introduced as depicted in Fig. 4 so as to transfer the excess power to the utility grid through the ILC whenever the surplus power produced in the PV system exceeds 10 kW. Without the selection switch, power would be absorbed by the SC bank.

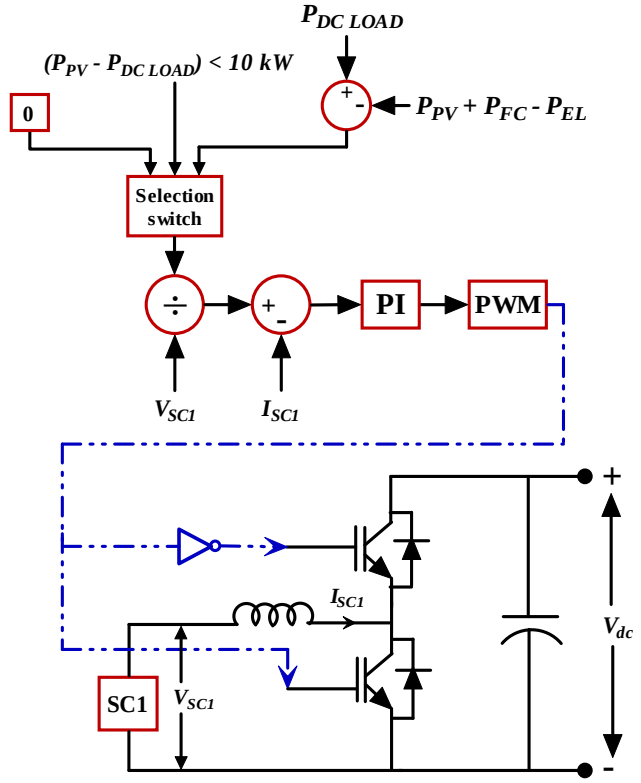

Figure 4. The control scheme for power smoothing in DC bus

D. Proposed Power Smoothing Method for the WECS

The power output of WECS is highly fluctuating due to continuously changing wind velocity. Since the WECS is coupled to the AC bus, it affects the operation of the DC subgrid and utility grid. If P_W is the actual power of WECS, P_{smooth} is the smooth power reference and V_{SC2} is the voltage of SC2, then the current reference to the SC bank is computed by equation (7):

$$I_{SC2(ref)} = \frac{P_{smooth} - P_W}{V_{SC2}} \tag{7}$$

A PI regulator is used to compute the duty ratio to the BDC based on the current output required from the SC system. The smoothing control technique developed for the WECS is depicted in Fig. 5.

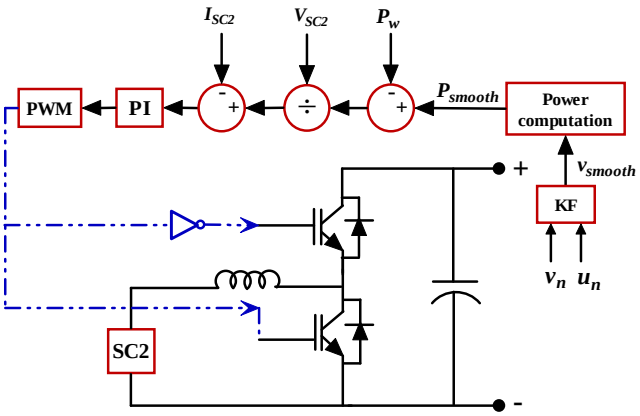

Figure 5. The control scheme for power smoothing of WECS by KFV approach

The KFV smoothing technique is developed to compute smooth power reference for power smoothing of the WECS. In the proposed approach, the intermittent wind velocity signal is processed by the KF to compute the smooth power reference. The KF is mainly used to estimate the state of the system when it contains random noises. This approach is inspired by the application of KF described in [25]. If x represents the state, z represents the output, w and m represent noises, the system equations are given by equations (8) and (9):

$$x_{n+1} = Ax_n + Bu_n + w_n \tag{8}$$

$$z_n = Hx_n + m_n \tag{9}$$

In this method, the wind velocity (v_n) and rate of change of v_n (a_n) are chosen as the state variables as represented in equation (10):

$$x_n = \begin{bmatrix} v_n \\ a_n \end{bmatrix} \tag{10}$$

If the rate of change of a_n is the input u_n to the system and T is the time for which the values are computed (2 µs), then the matrices are given by equation (11) and (12):

$$x_{n+1} = \begin{bmatrix} 1 & T \\ 0 & 1 \end{bmatrix} x_n + \begin{bmatrix} 0 \\ T \end{bmatrix} u_n \tag{11}$$

$$z_n = \begin{bmatrix} 1 & 0 \end{bmatrix} x_n \tag{12}$$

The prediction equations of the KF can be expressed by equations (13) and (14):

$$\hat{x}_n^- = A\hat{x}_{n-1} + Bu_{n-1} \tag{13}$$

$$P_n^- = AP_{n-1}A^T + Q_k \tag{14}$$

The correction equations [25-26] of the KF can be expressed by equations (15), (16) and (17):

$$K_n = P_n^- H^T (HP_n^- H^T + R_k)^{-1} \tag{15}$$

$$\hat{x}_n = \hat{x}_n^- + K_n(z_n - H\hat{x}_n^-) \tag{16}$$

$$P_n = (I - K_n H)P_n^- \tag{17}$$

where, P_n^- and P_n are the priori and posterior estimate error covariance, respectively. K_n is the Kalman gain; R_k and Q_k are measurement noise covariance and process noise covariance, respectively.

Based on the smoothened velocity (v_{smooth}), the smooth power reference for the WECS (P_{smooth}) is computed based on equation (18):

$$P_{smooth} = \frac{1}{2}\rho A v_{smooth}^3 C_p \eta \tag{18}$$

where, ρ is the density of air (1.225 kg/m^3), A is the swept area of the rotor blades, C_p is the coefficient of performance and η represents the average efficiency of generator and power conversion system (0.85). The maximum value of C_P is 0.47 [14]. The values of R_k and Q_k are carefully selected to ensure smooth power output without resulting in a larger difference between the smooth power and actual power. In this method, $Q_k = \begin{bmatrix} 10^{-12} & 0 \\ 0 & 10^{-12} \end{bmatrix}$ and $R_k = 10^3$.

The proposed KFV approach is compared with the rate-limiter-mean (RL-mean) method, LPF method and Kalman filter based weighted average (KFWA) method.

In the RL-mean approach, the fluctuating power output of WECS is passed through the rate limiter and then the average is computed using the 'mean' block of Simulink library [14].

In the LPF based method, smooth power is computed using a low pass filter [12]. The time period corresponding to LPF is chosen as 0.6 s.

In the KF based weighted average approach, the fluctuating output of WECS is used to compute maximum and minimum power for a certain time interval based on which, the weighted average is computed. The KF uses weighted average to calculate the desired power for smoothing [17-18].

IV. Results and Discussion

The practical data of irradiance and wind velocity for 10 minutes presented in [14] is chosen for analysis. The simulation is performed in MATLAB/Simulink software by scaling down the time to 6 s. The irradiation and wind velocity are illustrated in Fig. 6 and Fig. 7, respectively.

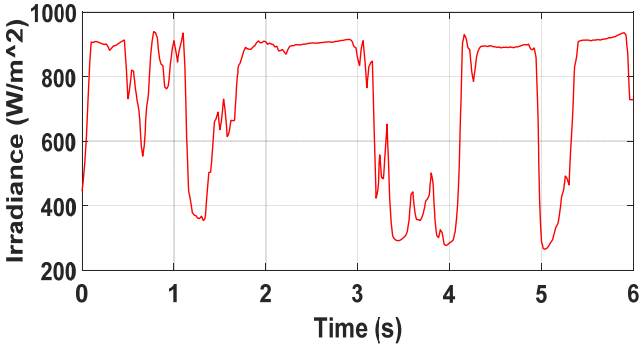

Figure 6. Irradiance

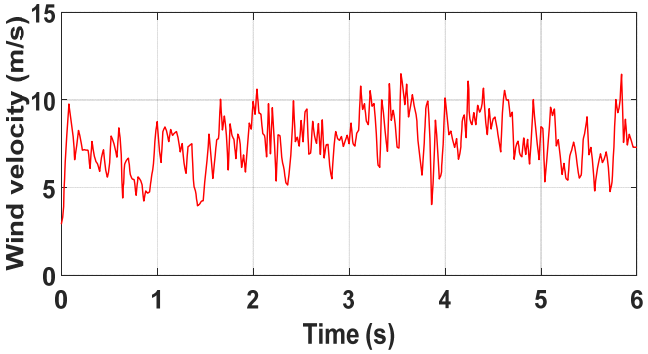

Figure 7. Wind velocity

A. Analysis of the HMG without Smoothing Controllers

The power balancing of the DC subgrid is achieved by EL and FC systems. Instantaneous power balancing on the DC subgrid is achieved by delivering or absorbing power through ILC (P_{EX}). FC system provides the power (P_{FC}) whenever there is a deficit in generation from PV array (P_{PV}). EL system absorbs power (P_{EL}) when the PV array produces excess power. When the power mismatch surpasses the capacity of FC or electrolyzer, the power balance is achieved with the help of AC subgrid. When the smoothing controller is not included in the system, P_{EX} is characterized by fluctuations that affect the power balance in the DC subgrid, as evident from Fig. 8.

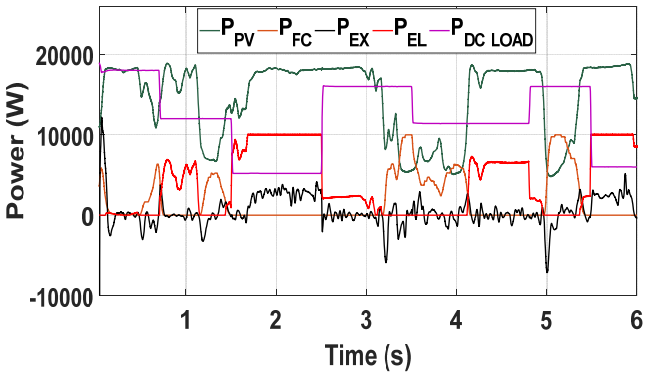

Figure 8. Power management of DC subgrid without smoothing controllers

The power management in the AC subgrid is depicted in Fig. 9. It can be observed that grid power is highly intermittent in the absence of smoothing controllers.

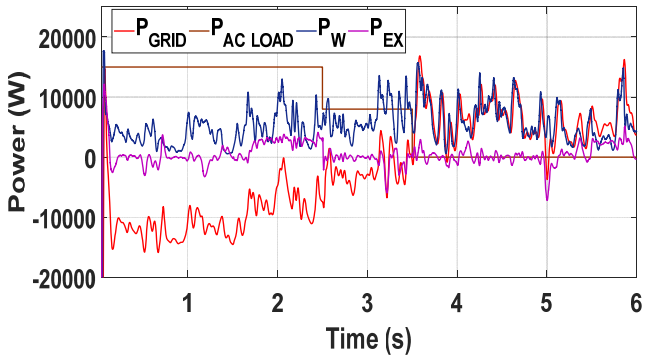

Figure 9. Power management of AC subgrid without smoothing controllers

B. Comparison of Smoothing Techniques for the WECS

The smooth power obtained by RL-mean, LPF, KFWA and proposed KFV technique are illustrated in Fig. 10. The maximum and minimum values of the power (P^{max} and P^{min}) are computed for certain duration and the smooth power variation rate (*SPVR*) [19] is computed as per equation (19).

The *SPVR* for different methods is presented in Fig. 11. The maximum and minimum *SPVR* for each method are presented in Table I. The smaller value of *SPVR* implies better power smoothing.

$$SPVR = \frac{P^{\max} - P^{\min}}{P^{rated}} \tag{19}$$

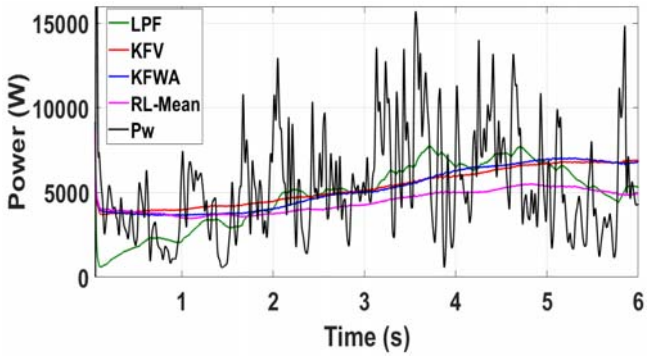

Figure 10. Fluctuating wind power and smooth powers

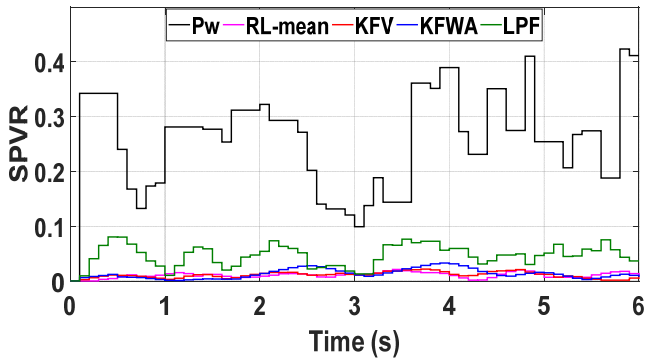

Figure 11. SPVR of fluctuating power and smooth power

TABLE I. SPVR FOR DIFFERENT METHODS

Method	SPVR (max)	SPVR (min)
LPF	0.080	0.009
RL-mean	0.021	0.001
KFWA	0.032	0.001
KFV	0.021	0.001

The moving average of the error between smooth power and fluctuating (actual) wind power is observed for each method as depicted in Fig. 12. It can be seen that the KF based methods provide a better estimate of smooth power as the moving average is close to zero. KFV approach is superior to other approaches.

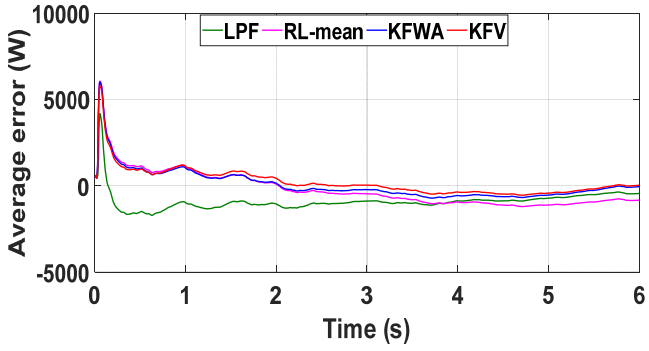

Figure 12. Moving average of the error

The SOC of SC2 with different smoothing techniques is illustrated in Fig. 13. It can be observed that when the LPF and RL-mean approaches are incorporated, SC bank operates more in the charging mode. However, when the KF

based approaches are incorporated, SC bank operates in both charge and discharge modes more evenly. This implies that the SC bank uniformly absorbs and delivers power to smoothen the power in KF based methods compared to other techniques. The proposed KFV method is found to be superior with respect to SOC.

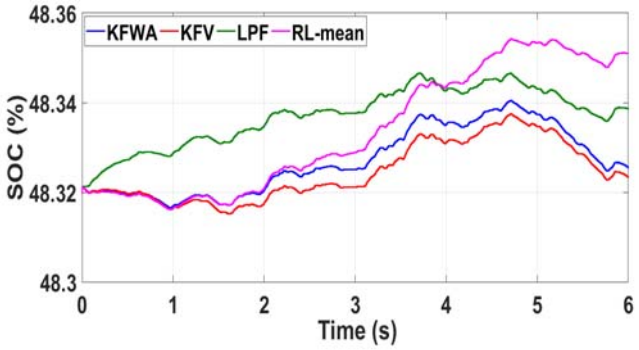

Figure 13. SOC of SC2 with different methods

The THD of the grid current obtained with different smoothing techniques is presented in Table II. THD is computed for ten cycles for the same interval of time for different cases. The THD is found to be low when the KFV method is incorporated for the SC bank in the WECS.

TABLE II. THD OBTAINED WITH DIFFERENT METHODS

Method	THD
LPF	4.1%
RL-mean	4.62%
KFWA	3.84%
KFV	3.68%

When various parameters such as SPVR, moving average of the error, SOC and THD are analyzed, the *proposed KFV method* is found to be superior. Hence it is chosen for smoothing the output of WECS.

C. Analysis of the Impact of Smoothing Controllers

The V_{dc} in the presence and absence of the smoothing controllers on both subgrids is illustrated in Fig. 14. The voltage deviations in the DC bus are considerably reduced with smoothing controllers.

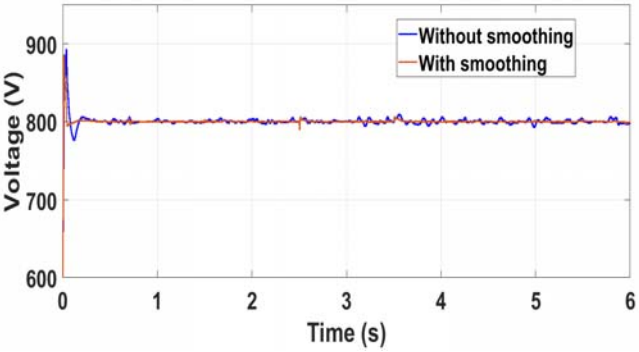

Figure 14. DC bus voltage with and without smoothing

The active power exchanged with the grid is shown in Fig. 15. Fluctuations in active power are reduced by incorporating the smoothing controller for WECS. Better smoothing is achieved when smoothing controllers are incorporated for both WECS and DC subgrid.

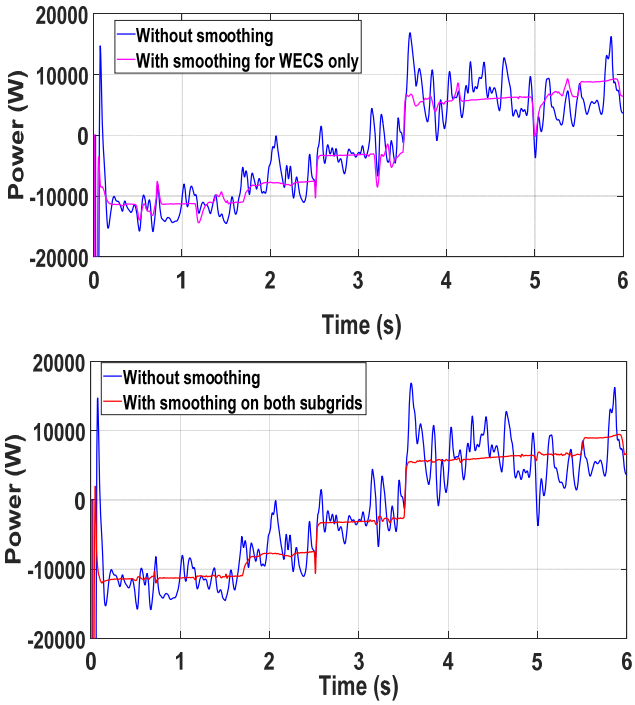

Figure 15. Active power exchanged with the grid

The reactive power exchanged with the grid is maintained zero as depicted in Fig. 16.

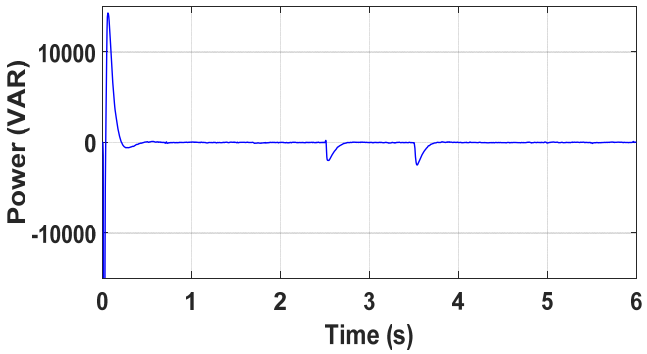

Figure 16. Reactive power

The power management in DC subgrid in the presence of smoothing controllers on both the subgrids is depicted in Fig. 17. The smoothing controller of the DC subgrid helps in the reduction of stress on the ILC.

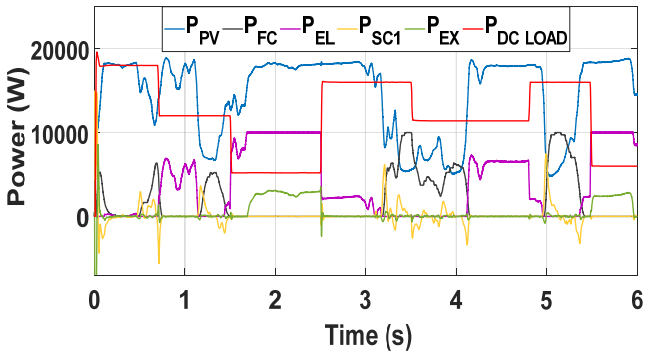

Figure 17. The power balance in DC subgrid with smoothing controllers

The power exchange via the ILC in the presence and absence of smoothing controllers is depicted in Fig. 18. Since immediate power balancing is achieved by SC1 and fluctuations in the output of WECS are reduced by SC2, the stress on ILC is significantly minimized.

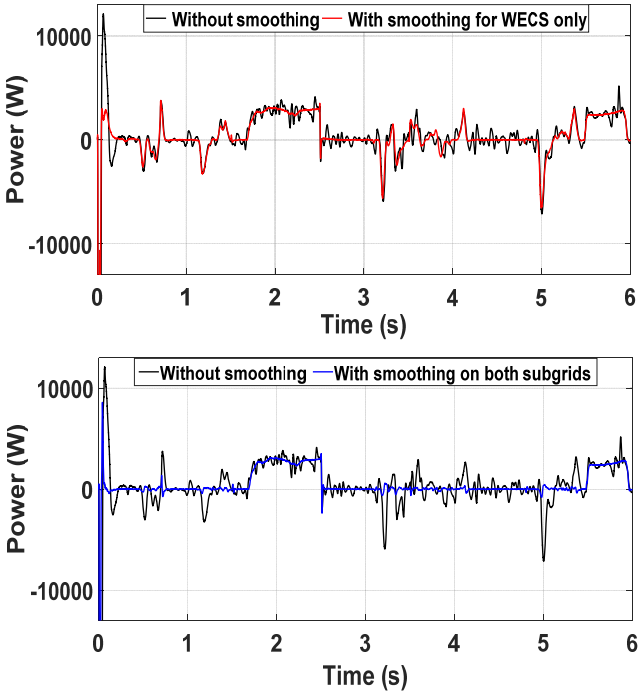

Figure 18. The power exchanged through ILC

The power balance equations on DC and AC subgrids in the absence of SC-based smoothing controllers are given by equations (20) and (21):

$$P_{PV} + P_{FC} - P_{EL} - P_{EX} = P_{DC\,LOAD} \quad (20)$$

$$P_{W} - P_{GRID} + P_{EX} = P_{AC\,LOAD} \quad (21)$$

The power balance equations on the DC and AC subgrids in the presence of smoothing controllers are given by equations (22) and (23):

$$P_{PV} + P_{FC} + P_{SC} - P_{EL} - P_{EX} = P_{DC\,LOAD} \quad (22)$$

$$P_{smooth} - P_{GRID} + P_{EX} = P_{AC\,LOAD} \quad (23)$$

If the power flowing through ILC (P_{EX}) is positive, the power is flowing from DC subgrid to AC subgrid and if it is negative, the power is drawn from AC subgrid. Similarly, if the grid active power (P_{GRID}) is positive, then the power is sent to the grid and if it is negative, the grid supplies the power.

The sinusoidal waveform of the grid current when the smoothing controllers are incorporated in the system is shown in Fig. 19. The current is less distorted. The harmonic spectrum of the grid current in the presence of the smoothing controller for SC1 and KFV based smoothing controller for SC2 is shown in Fig. 20. The THD is within acceptable limits (lesser than 5%).

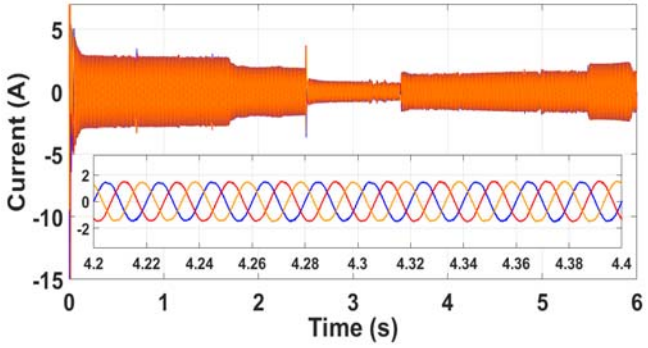

Figure 19. Grid current

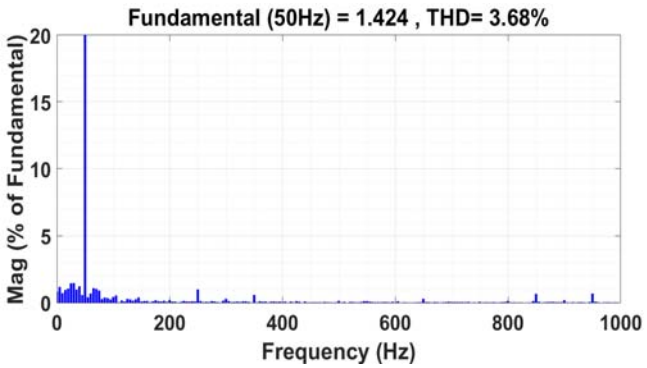

Figure 20. Harmonic spectrum of grid current

V. Conclusion

This paper presents a novel power smoothing technique for the grid integrated HMG with PV, WECS and FC based DG system. Distinct power smoothing control schemes are employed on AC and DC subgrids. The SC system is controlled to absorb and deliver power during sudden power deviations on DC subgrid. The output power of WECS coupled to the AC subgrid is smoothened using the SC system by different smoothing techniques. The key findings of this study are summarized below.

- When PV array or WECS are integrated on both AC and DC subgrids, intermittent power production affects the power and voltage profiles of both subgrids.
- KF based velocity smoothing approach is found to be effective in smoothing the power output for WECS.
- By incorporating the smoothing controller developed for the DC subgrid along with the smoothing controller for WECS, stress on the ILC is significantly minimized.
- The smoothing controllers developed in this work have reduced the stress on the individual subgrids and the utility grid; thereby, the power quality is enhanced.

List of Abbreviations

BES	Battery Energy Storage
EL	Electrolyzer
FC	Fuel Cell
HMG	Hybrid AC-DC Microgrid
ILC	Interlinking Converter
KF	Kalman Filter
KFV	Kalman Filter Based Velocity Smoothing
KFWA	Kalman Filter Based Weighted Average
LPF	Low Pass Filter
MG	Microgrid
MPPT	Maximum Power Point Tracking
PMSG	Permanent Magnet Synchronous Generator
PV	Photovoltaic
SC	Supercapacitor
SOC	State of Charge
SPVR	Smooth Power Variation Rate
THD	Total Harmonic Distortion
WECS	Wind Energy Conversion System

References

[1] P. Wang, X. Liu, C. Jin, P. Loh, and F. Choo, “A hybrid AC/DC micro-grid architecture, operation and control,” in IEEE Power and Energy Society General Meeting, Jul. 2011, pp. 1–8. doi:10.1109/PES.2011.6039453

[2] X. Liu, P. Wang, and P. C. Loh, "A hybrid AC/DC microgrid and its coordination control," IEEE Transactions on Smart Grid, vol. 2, no. 2, pp. 278–286, Jun. 2011. doi:10.1109/TSG.2011.2116162

[3] F. Nejabatkhah and Y. W. Li, "Overview of power management strategies of hybrid AC/DC microgrid," IEEE Transactions on Power Electronics, vol. 30, no. 12, pp. 7072–7089, Dec. 2015. doi:10.1109/TPEL.2014.2384999

[4] F. Blaabjerg, R. Teodorescu, M. Liserre, and A. V. Timbus, "Overview of control and grid synchronization for distributed power generation systems," IEEE Transactions on Industrial Electronics, vol. 53, no. 5, pp. 1398–1409, Oct. 2006. doi:10.1109/TIE.2006.881997

[5] T. D. Hund, S. Gonzalez, and K. Barrett, "Grid-tied PV system energy smoothing," in Conference Record of the IEEE Photovoltaic Specialists Conference, Jun. 2010, pp. 2762–2766. doi:10.1109/PVSC.2010.5616799

[6] J. Pegueroles-Queralt, F. D. Bianchi, and O. Gomis-Bellmunt, "A power smoothing system based on supercapacitors for renewable distributed generation," IEEE Transactions on Industrial Electronics, vol. 62, no. 1, pp. 343–350, Jan. 2015. doi:10.1109/TIE.2014.2327554

[7] C. Ceja-Espinosa and E. Espinosa-Juárez, "Smoothing of photovoltaic power generation using batteries as energy storage," in IEEE PES Innovative Smart Grid Technologies Conference - Latin America, ISGT Latin America, Sep. 2017, pp. 1–6. doi:10.1109/ISGT-LA.2017.8126758

[8] A. M. Howlader, N. Urasaki, A. Yona, T. Senjyu, and A. Y. Saber, "A review of output power smoothing methods for wind energy conversion systems," Renewable and Sustainable Energy Reviews, vol. 26, pp. 135–146, Oct. 2013. doi:10.1016/j.rser.2013.05.028

[9] H. Lee, M. Hwang, E. Muljadi, P. Sørensen, and Y. C. Kang, "Power-smoothing scheme of a DFIG using the adaptive gain depending on the rotor speed & frequency deviation," Energies, vol. 10, no. 4, p. 555, Apr. 2017. doi:10.3390/en10040555

[10] X. Li, D. Hui, and X. Lai, "Battery energy storage station (BESS)-based smoothing control of photovoltaic (PV) and wind power generation fluctuations," IEEE Transactions on Sustainable Energy, vol. 4, no. 2, pp. 464–473, Apr. 2013. doi:10.1109/TSTE.2013.2247428

[11] G. Mandic, A. Nasiri, E. Ghotbi, and E. Muljadi, "Lithium-ion capacitor energy storage integrated with variable speed wind turbines for power smoothing," IEEE Journal of Emerging and Selected Topics in Power Electronics, vol. 1, no. 4, pp. 287–295, Dec. 2013. doi:10.1109/JESTPE.2013.2284356

[12] M. R. I. Sheikh and N. Mondol, "Wind power smoothing scheme using SMES with reduced capacity," in International Conference on Informatics, Electronics and Vision, ICIEV, May 2012, pp. 404–410. doi:10.1109/ICIEV.2012.6317425

[13] X. Han, F. Chen, X. Cui, Y. Li, and X. Li, "A power smoothing control strategy and optimized allocation of battery capacity based on hybrid storage energy technology," Energies, vol. 5, no. 5, pp. 1593–1612, May 2012. doi:10.3390/en5051593

[14] N. S. Jayalakshmi and D. N. Gaonkar, "A new control method to mitigate power fluctuations for grid integrated PV/wind hybrid power system using ultracapacitors," International Journal of Emerging Electric Power Systems, vol. 17, no. 4, pp. 451–461, Aug. 2016. doi:10.1515/ijeeps-2015-0183

[15] R. Sharma and S. Suhag, "Supercapacitor utilization for power smoothening and stability improvement of a hybrid energy system in a weak grid environment," Turkish Journal of Electrical Engineering & Computer Sciences, vol. 26, no. 1, pp. 347–362, Jan. 2018. doi:10.3906/elk-1703-101

[16] M. Y. Worku and M. A. Abido, "Fault ride-through and power smoothing control of PMSG-Based wind generation using supercapacitor energy storage system," Arabian Journal for Science and Engineering, vol. 44, no. 3, pp. 2067–2078, Mar. 2019. doi:10.1007/s13369-018-3284-1

[17] D. Lamsal, V. Sreeram, and Y. Mishra, "Reducing power fluctuations from wind and photovoltaic systems using discrete Kalman filter," in Australasian Universities Power Engineering Conference (AUPEC), Sep. 2016, pp. 1–5. doi:10.1109/aupec.2016.7749297

[18] D. Lamsal, V. Sreeram, Y. Mishra, and D. Kumar, "Achieving a minimum power fluctuation rate in wind and photovoltaic output power using discrete kalman filter based on weighted average approach," IET Renewable Power Generation, vol. 12, no. 6, pp. 633–638, Jan. 2018. doi:10.1049/iet-rpg.2017.0346

[19] D. Lamsal, V. Sreeram, Y. Mishra, and D. Kumar, "Output power smoothing control approaches for wind and photovoltaic generation systems: A review," Renewable and Sustainable Energy Reviews, vol. 113, p. 109245, Oct. 2019. doi:10.1016/j.rser.2019.109245

[20] N. S. Jayalakshmi, D. N. Gaonkar, and P. B. Nempu, "Power control of PV/fuel cell/supercapacitor hybrid system for stand-alone applications," International Journal of Renewable Energy Research, vol. 6, no. 2, pp. 672–679, Jun. 2016

[21] M. Uzunoglu, O. C. Onar, and M. S. Alam, "Modeling, control and simulation of a PV/FC/UC based hybrid power generation system for stand-alone applications," Renewable Energy, vol. 34, no. 3, pp. 509–520, Mar. 2009. doi:10.1016/j.renene.2008.06.009

[22] T. Schucan, "Case studies of integrated hydrogen systems," IEA Hydrogen Implementing Agreement, Final report for Subtask A of Task. 11, Dec. 1999

[23] A. Reznik, M. G. Simoes, A. Al-Durra, and S. M. Muyeen, "LCL Filter design and performance analysis for grid-interconnected systems," IEEE Transactions on Industry Applications, vol. 50, no. 2, pp. 1225–1232, Mar. 2014. doi:10.1109/TIA.2013.2274612

[24] K. Tatjana "Control of voltage source converters for power system applications," Master's thesis, Norwegian University of Science and Technology, 2011

[25] D. Simon, "Kalman filtering," Embedded systems programming, vol. 14, no. 6, pp. 72–79, Jun. 2001

[26] G. Welch and G. Bishop, An Introduction to the Kalman filter, pp. 1–16, Jul. 2006